Available online at www.sciencedirect.com
ScienceDirect
Journal of Solid State Chemistry 180 (2007) 3521–3528
JOURNAL OF SOLID STATE CHEMISTRY
www.elsevier.com/locate/jssc

First-principles study of structural and vibrational properties of crystalline silver azide under high pressure

Weihua Zhu*, Heming Xiao*

Department of Chemistry, Institute for Computation in Molecular and Materials Science, Nanjing University of Science and Technology, Nanjing 210094, China

Received 2 September 2007; received in revised form 11 October 2007; accepted 14 October 2007
Available online 22 October 2007

Abstract

A detailed first-principles study of the structural and vibrational properties of crystalline silver azide under hydrostatic pressure of 0–500 GPa has been performed with density functional theory in the generalized gradient approximation. The crystal structure is relaxed to allow ionic configurations, cell shape, and volume to change without any symmetry constraints. It is found that the silver azide crystal remains orthorhombic structure with *Ibam* space group for pressures up to 7 GPa, where there is a transition to an *I*4/*mcm* tetragonal symmetry. The lattice parameter and electronic structure are investigated as functions of pressure. The calculated vibrational frequencies at ambient pressure are in agreement with available experimental data. We also discuss the pressure-induced frequency shifts for the internal and lattice modes of silver azide crystal upon compression.

Keywords: Density functional theory; Hydrostatic pressure; Density of states; Vibrational properties

1. Introduction

Silver azide (AgN_3) is a sensitive primary explosive. When subjected to a suitable stimulus such as impact, heat, friction, or electric discharge, it is able to explode. Therefore, there has been a significant history of interest in its structural and explosive properties since it was first isolated and recognized as a primary explosive [1–25].

Materials such as propellants and explosives contain tightly bonded groups of atoms that retain their molecular character until a sufficient stimulus is applied to cause exothermic dissociation. This in turn triggers further dissociation leading to initiation or ignition. The macroscopic behavior is ultimately controlled by microscopic properties such as the electronic structure and interatomic forces. Thus, a desire to probe more fundamental questions relating to the basic properties of AgN_3 as a solid energetic material is generating significant interest in the basic solid-state properties of such energetic system. Although the detailed decomposition mechanism by which AgN_3 releases energy under mechanical shock is still not well understood, it has been suggested that its decomposition may result from transferring thermal and mechanical energy into the internal degrees of freedom of tightly bonded groups of atoms in solid [26–28]. Therefore, the knowledge of its electronic and vibrational properties appears to be very important in understanding its explosive properties.

The investigation of the microscopic properties of energetic materials, which possess a complex chemical behavior, remains to be a challenging task. An important challenge for experiment measurements is to predict the pressure effects in explosive materials under extreme conditions. Pressure is an important variable that can be used to tune physical properties. Rees and Chaudhri [14] have performed an experimental study to investigate the electrical conductivity of AgN_3 at hydrostatic pressures of up to 4 GPa. However, there is great difficulty in determining compressibility of the explosive materials under extreme condition because it is unstable and explosive. An alternative approach is atomistic simulation, an effective way to model the physical and chemical properties of complex solids at the atomic level as a

*Corresponding authors. Fax: +86 25 84303919.
E-mail addresses: zhuwh@mail.njust.edu.cn (W. Zhu), xiao@mail.njust.edu.cn (H. Xiao).

0022-4596/$ - see front matter © 2007 Elsevier Inc. All rights reserved.
doi:10.1016/j.jssc.2007.10.016

complement to experimental work. Recently, density functional theory (DFT) method with pseudopotentials and a plane-wave basis set, often used within the generalized gradient approximation (GGA), has been well established and has been successfully applied to the study of structures and properties of solids under hydrostatic compression effect [29,30]. The structures and vibrational properties under high-pressure condition is necessary to understanding the high-pressure behavior and initiation process of the explosives, so a detail high-pressure study on AgN_3 is necessary.

In this study, we performed periodic DFT calculations to study the structural and vibrational properties of AgN_3 under different pressures. The atomic positions and the unit-cell parameters were allowed to relax to the minimum energy configuration to investigate the crystal structure at different pressures. Next, we examined the variations in the electronic structure under compression. Finally, we discussed the pressure effects on the vibrational properties.

The remainder of this paper is organized as follows. A brief description of our computational method is given in Section 2. The results and discussion are presented in Section 3, followed by a summary of our conclusions in Section 4.

2. Computational method

The calculations performed in this study were done based on DFT [31] with Vanderbilt-type ultrasoft pseudopotentials [32] and a plane-wave expansion of the wave functions. The self-consistent ground state of the system was determined by using a band-by-band conjugate gradient technique to minimize the total energy of the system with respect to the plane-wave coefficients. The electronic wave functions were obtained by a density-mixing scheme [33] and the structures were relaxed by using the Broyden, Fletcher, Goldfarb, and Shannon method [34]. The GGA proposed by Perdew and Wang [35,36], named PW91, was employed. The cutoff energy of plane waves was set to 500.0 eV. Brillouin zone sampling was performed by using the Monkhost–Pack scheme with a k-point grid of $4 \times 4 \times 4$. The values of the kinetic energy cutoff and the k-point grid were determined to ensure the convergence of total energies.

The experimental crystal structure of AgN_3 [37,38] was first relaxed to allow the ionic configurations, cell shape, and volume to change at ambient pressure. Then from this relaxed structure, we applied hydrostatic compression of 1–500 GPa. In the geometry relaxation, the total energy of the system was converged less than 2.0×10^{-5} eV, the residual force less than 0.05 eV Å^{-1}, the displacement of atoms less than 0.002 Å, and the residual bulk stress less than 0.1 GPa. For all the equilibrium structures, the Mulliken populations were investigated using a projection of the plane-wave states onto a linear combination of atomic orbitals basis set [39,40], which is widely used to perform charge transfers and populations analysis. The phonon frequencies at the gamma point have been calculated from the response to small atomic displacements [41].

3. Results and discussion

3.1. Crystal structures

In our previous study [42], we applied two different functionals (LDA and GGA) to bulk lithium azide as a test and found that the GGA (PW91) approximation may be expected to produce more reliable predictions of the structures. Therefore, GGA was used in all calculations here. The effect of pressure on the lattice constants of AgN_3 is shown in Fig. 1. We note that the largest compression of the unit cell takes place in the region of low pressures below 7 GPa, where the compressibility is anisotropic. The structure is much stiffer in the a direction than along the b and c axes. Above this pressure, the lattice parameters decrease monotonically with the increment of pressure. It is also found that with increasing pressure from 7 GPa the lattice constants a and b become equal; moreover, the lattice constant c versus pressure curve crosses the a and b versus pressure ones at about 500 GPa. This indicates that there may be a transition of crystal symmetry. Fig. 2 displays the variation of the unit cell angles with increasing pressure. In the low-pressure range from 0 to 7 GPa, the deviations of the unit cell angles from 90.0° remains very small. The overall crystal symmetry remains orthorhombic *Ibam* space group in this pressure region. Over this pressure range, the unit cell angles remain unchanged. The crystal symmetry is changed from orthorhombic to *I*4/*mcm* tetragonal symmetry.

It is interesting to note that the crystal structure of AgN_3 under pressures up to 500 GPa only experiences a phase transition at pressure above 7 GPa and shows high stability. However, recent experimental high-pressure studies of sodium azide (NaN_3) [43] have shown that this substance undergoes a set of phase transitions at pressures up to 120 GPa including the transition involving the formation of polynitrogen networks at pressure above 100 GPa. The differences in their stability under the effect of pressures may be understood on the basis of electronic structure. NaN_3 at ambient pressure is an ionic compound, in which the peaks originating from the sodium states hardly overlap these arising from the N-states in the valence band region of density of states (DOS) [44], while AgN_3 has some covalent character, in which there is hybridization between the Ag and end N atoms [45]. Therefore, the crystal structure of the former is easier to change than that of the latter under the influence of pressures. A possible arrangement of azide ions for NaN_3 at high pressure is a collapse into a planar net with perpendicularly oriented ions, whereas, in this structure, AgN_3 remains a molecular crystal [46].

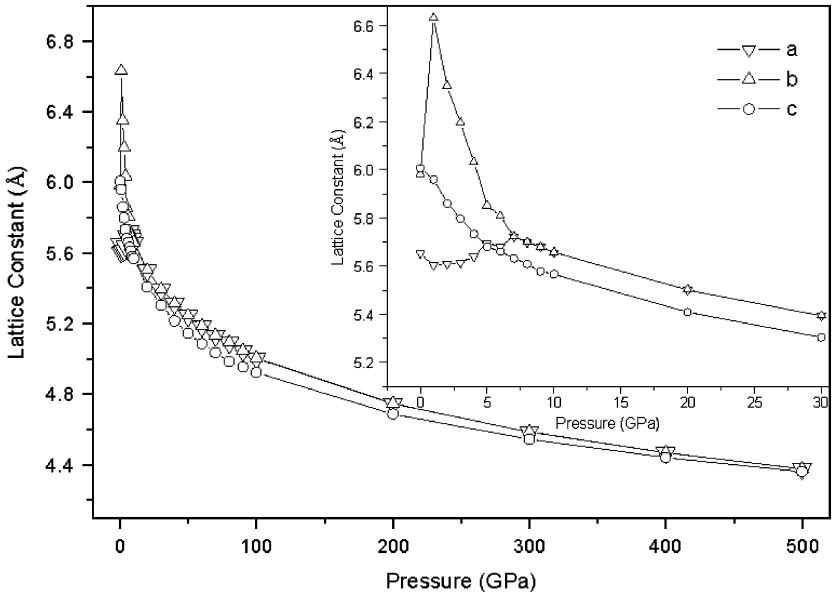

Fig. 1. Lattice constants as a function of hydrostatic pressure for AgN_3.

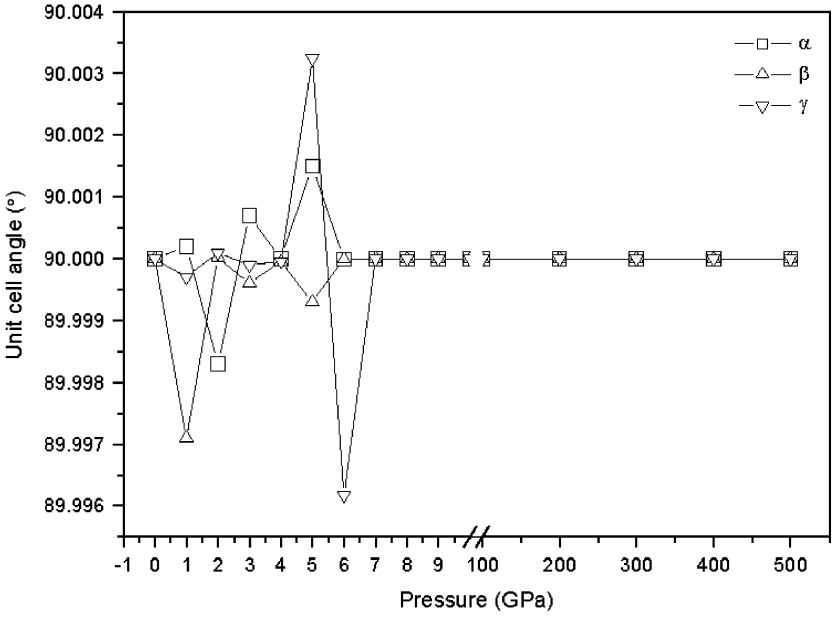

Fig. 2. Unit cell angles as a function of hydrostatic pressure for AgN_3.

3.2. Electronic structures

Band gap is an important parameter to characterize the electronic structure of solids. The effect of pressure on the band gaps of AgN_3 is shown in Fig. 3. In the region of low pressures below 10 GPa, the band gap of AgN_3 remains hardly changed. With further increment of pressure, the band gap gradually decreases. Rees and Chaudhri [14] have performed experimental studies to investigate the influences of hydrostatic pressure on the electrical conductivity of AgN_3. The results show that the electrical conductivity decreases continually as the pressure increases up to about 4 GPa. This may be because the band gap of AgN_3 has not been reduced enough to give rise to an electronic component to the conduction current. The view is supported by our calculated result that AgN_3 in the pressure range of 0–10 GPa have almost the same bad gap. However, with further increment of pressure, the band gap of AgN_3 continuously reduces, so its electrical conduction may result from the electronic contribution. It may be inferred that the electrical conductivity of AgN_3 will increase with the increment of pressure from 10 GPa. Since AgN_3 is an ionic crystal, the applied compression plays little effect on the intermolecular spacing but leads to significant influence on the intramolecular geometry. This is supported below by the variations in the bond order of

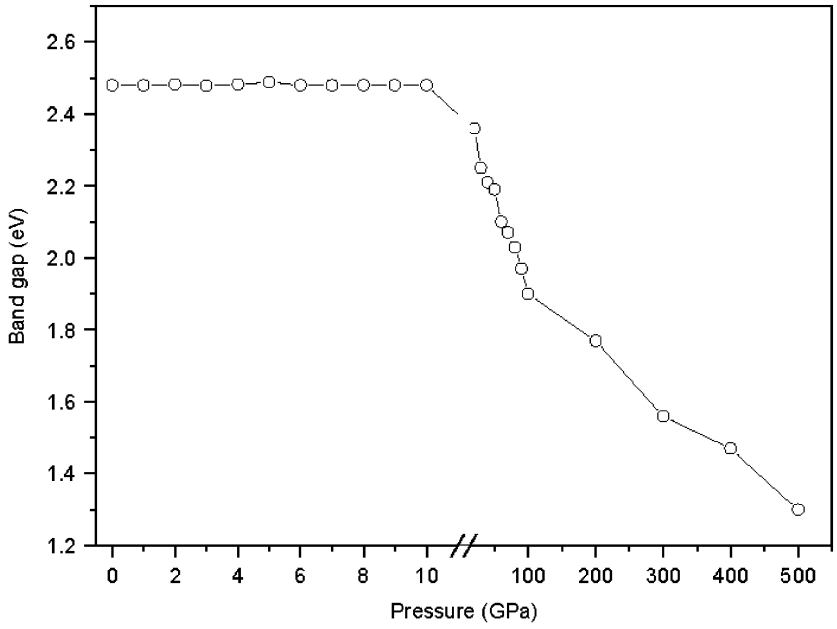

Fig. 3. Band gaps as a function of hydrostatic pressure for AgN_3.

the end N-central N bond and vibrational property under compression.

To obtain further information about the bond nature of AgN_3 at the different pressures the calculated total DOS and partial DOS (PDOS) are displayed in Fig. 4. First, the DOS peak in the upper valence band becomes more and more dispersed with increasing pressure. This shows that the electronic delocalization in AgN_3 gradually increases under the influence of pressure. Second, upon compression the gap between conduction and valence bands gradually decreases. This suggests that the electrical conductivity increase continually. Finally, there is the increase of charge overlap in the system with increasing pressure.

The atom-resolved DOS and PDOS of AgN_3 at different pressures are also shown in Fig. 4. The main features can be summarized as follows: (i) The overlaps between the Ag- and N-states continuously increase with increasing pressure. (ii) In the low-pressure region, some peaks originating from the Ag-states overlap these arising from the N-states in the valence band region of DOS, which does suggest that there is hybridization between silver and nitrogen atoms. However, in the high-pressure region, all the peaks in this valence band region originate from the Ag- and N-states. This means that the interactions between electrons are enhanced. (iii) On the whole, the PDOS of AgN_3 is identical with that of its azide ion in the low-pressure region, implying that the modifications in the DOS are mainly due to the changes in the PDOS of Ag-states, whereas the case is quite the contrary in the high-pressure region.

Finally, we try to correlate the AgN_3's stabilities (or explosive characters) under compression with the electronic structure. As can be seen in Fig. 3, the band gap of AgN_3 gradually decreases with the increment of pressure. The smaller the band gap is, the easier the electron transfers from valence band to conduction band, and the more the AgN_3 becomes decomposed and exploded [18,19]. Therefore, it is concluded that the impact sensitivity for AgN_3 becomes more and more sensitive with the increment of pressure. In several papers [47–50], Gilman has emphasized the role of highest occupied molecular orbital–lowest unoccupied molecular orbital (HOMO–LUMO) gap closure in molecules suffering shear strain. Further reports [51,52] on the excitonic mechanism of detonation initiation show that the pressure inside the impact wave front reduces the band gap between valence and conducting bands and promotes the HOMO–LUMO transition within a molecule. These studies have suggested that the HOMO–LUMO gap in molecules suffering shear strain, impact wave, or distortion relates directly to the sensitivity. This further supports our conclusion here.

The variations in the stability for AgN_3 under compression can be further explained by the information contained in the DOS. The thermal decomposition of a number of simple azides results in the formation of metal and nitrogen. For AgN_3, the rate-determining step in its thermal decomposition is the thermal excitation of an electron to the conduction band [4]. The initial step in the decomposition can therefore be represented as

$$N_3^- \rightleftarrows N_3 + e. \quad (1)$$

Nitrogen gas will be formed by the reaction of two azide radicals at the surface. Metal silver will be formed according to the mechanism suggested by Mitchell [46]:

$$Ag_n + Ag^+ + e \rightarrow Ag_{n+1} \quad (n>2). \quad (2)$$

Therefore, the decomposition of the azides depends on the formation of neutral azide radicals giving rise to a

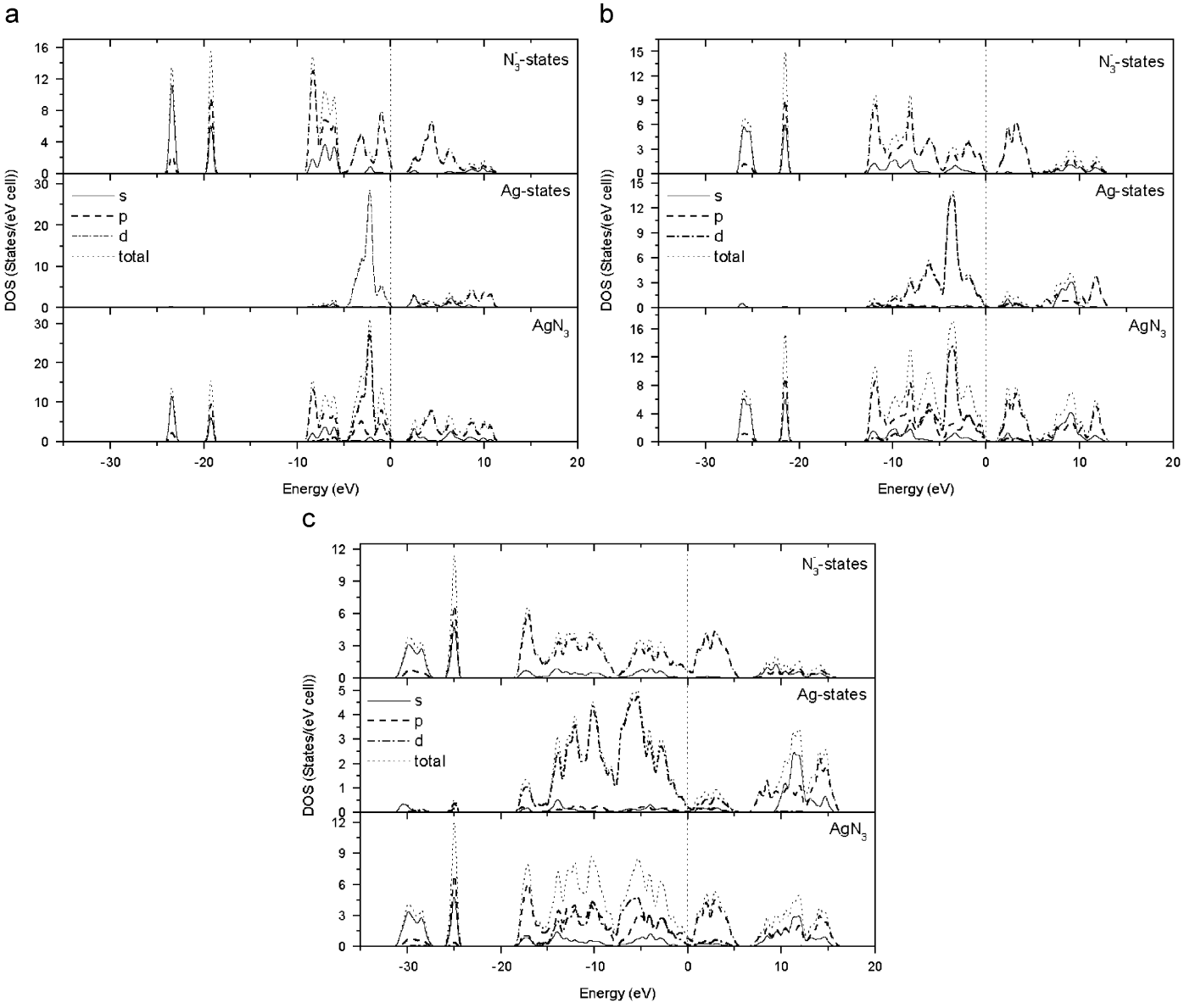

Fig. 4. Total and partial density of states (DOS) of AgN_3 at different hydrostatic pressures: (a) 6 GPa; (b) 100 GPa; (c) 500 GPa. The Fermi energy is shown as a vertical dashed line.

surface reaction. The more intimately the valence electron is under the influence of the metal, the more the azide group tends to the optimum condition of neutrality, and the easier the thermal decomposition of the metal azide becomes. From Fig. 4, we note that the PDOS peak in the upper valence band from Ag-states becomes more and more dispersed with increasing pressure. This indicates that the effects of the Ag-states on the valence electrons of the azide group become more and more obvious under compression, so the azide group gradually tends to the optimum condition of neutrality. That is, the stability for the formation of neutral azide radicals for AgN_3 increases gradually with increasing pressure. Therefore, the activation order for thermal decomposition of AgN_3 under compression follows the increase in the stability of their neutral azide radicals. From these suggestions, we may infer that the impact sensitivity for AgN_3 gets more and more sensitive with the increment of pressure.

3.3. Vibrational properties

In this section, we turn to investigate the vibrational frequencies for crystal AgN_3 under hydrostatic pressure. Both the internal modes due to intramolecular interactions and the lattice modes due to intermolecular interactions were considered here. Table 1 presents the calculated vibrational frequencies for AgN_3 at zero pressure together with the experimental values [53,54]. The internal modes are indexed as V1–V5 and the lattice modes as L1–L12. The results show that the calculated and measured frequencies are in reasonable agreement. We should note that our calculations are performed at zero temperature

Table 1
Vibrational frequencies (cm^{-1}) for the lattice and internal modes of crystalline silver azide

Mode	Assignment	This work	Experiment	
			Ref. [53]	Ref. [54]
L1	Translational vibration	48.3	44	
L2	Translational vibration	48.8	53	
L3	Translational vibration	60.8	58	
L4	Translational vibration	64.1	60	
L5	Translational vibration	64.8	70	
L6	Rotational lattice vibration	69.3	74	
L7	Translational vibration	130.1	130	
L8	Rotational lattice vibration	161.2	160	160
L9	Translational vibration	184.1	180	
L10	Rotational lattice vibration	191.9	189	
L11	Rotational lattice vibration	216.3	220	
L12	Translational vibration	264.5	230	
V1	N_3 bending	608.9	618	599
V2	N_3 symmetric stretching + translational vibration	1407.8	1402	1331
V3	N_3 symmetric stretching + translational vibration	1410.0	1415	
V4	N_3 asymmetric stretching	2157.8	2144	2000
V5	N_3 asymmetric stretching	2183.1	2187	

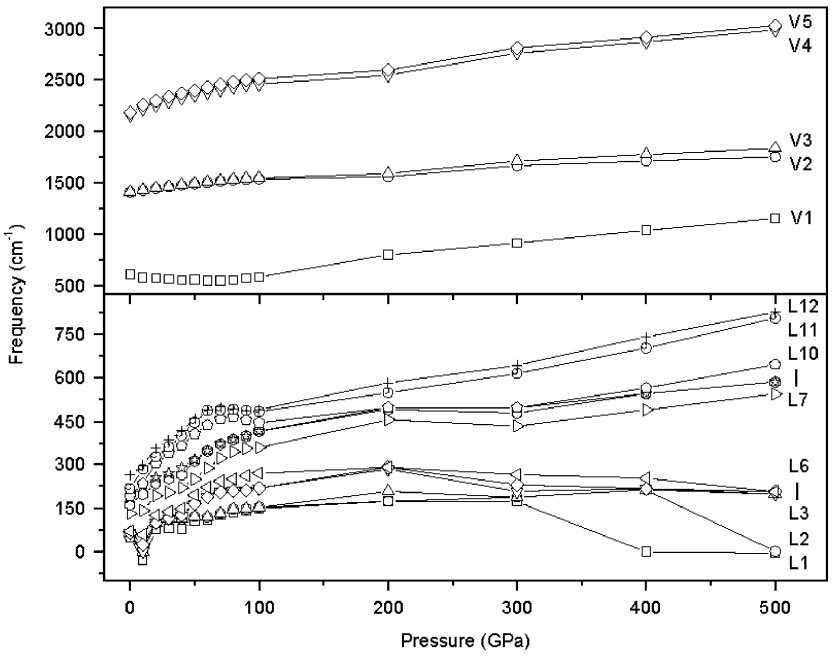

Fig. 5. Pressure-induced shifts of vibrational frequencies for the internal modes V1–V5 and lattice modes L1–L12 for AgN_3.

but the experimental measures were recorded at 80 K [53], so the direct comparison between the calculated and measured data will result in the discrepancies. In addition, the DFT–GGA approximation considered in this work is not able to reproduce intermolecular interaction very well, therefore, the calculated frequencies for the lattice modes have larger deviations from the experiment values than those for the internal modes.

Fig. 5 displays the pressure dependence of vibrational frequencies of AgN_3 under hydrostatic compression. As the pressure increases, the vibrational frequencies of the internal modes V1–V5 increase monotonically (so-called mode hardening) except that the N_3 bending mode (V1) shows clear minima at pressure about 50 GPa. This indicates that the intramolecular bonding strength enhances under compression, which is in agreement with the increase of the bond order of the end N-central N bond shown in Fig. 6. Such consistency between the frequency shifts of the internal modes and the variation of bond order indicates there is a correlation between the structural and spectroscopic properties of energetic solids under compression. The evolution of the lattice modes with increasing

pressure is slightly different from that of the internal modes. With the increase of pressure, the vibrational frequencies of the lattice modes L7–L12 increase continually, whereas those of the lattice modes L1–L6 presents another variation pattern: they first increase, peak at one pressure, and then decease. Fig. 7 presents the coefficients for pressure-induced shifts of vibrational frequencies of the internal modes and lattice modes for AgN_3 from the linear fit of the frequency versus pressure data in the pressure range of 0–500 GPa. It is obvious that different vibrational modes show distinctly different pressure-dependent behaviors. The two modes V4 and V5 associated with N_3 asymmetric stretching exhibit the most significant shift and their fitted coefficients are $1.5\,cm^{-1}\,GPa^{-1}$. This indicates that the N–N bond is the most compressible bond in AgN_3. In addition, the N_3 bending mode V1 shows a pronounced shift with a coefficient of $1.3\,cm^{-1}\,GPa^{-1}$. With increasing pressure, the two modes L11 and L12 present the most frequency shifts among the lattice modes and their coefficients are 0.93 and $0.95\,cm^{-1}\,GPa^{-1}$, respectively. These observations reflect that the pressure-induced frequencies increase of the internal modes is much more pronounced than those for the lattice modes. This shows that the hydrostatic compression produces a more significant influence on the intramolecular interaction than on the intermolecular interaction.

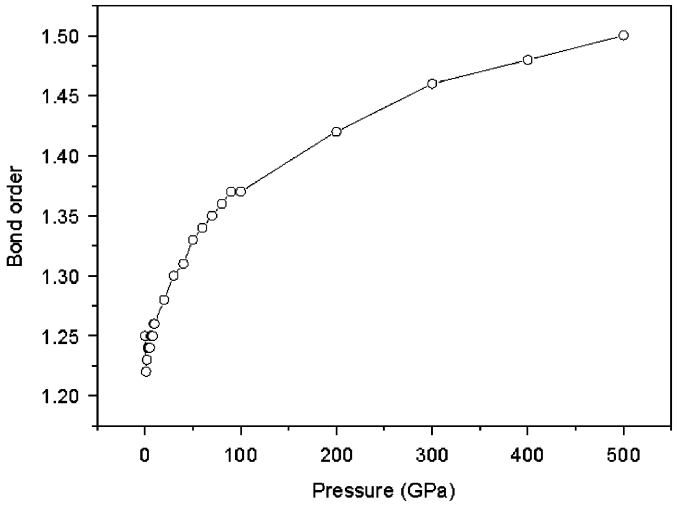

Fig. 6. Bond order of end N-central N bonds in AgN_3 as a function of hydrostatic pressure.

4. Conclusions

In this study, we have performed a detailed first-principles study of the structural and vibrational properties of crystalline AgN_3 under hydrostatic pressure of 0–500 GPa within DFT in the GGA. It is found that the AgN_3 crystal remains orthorhombic structure with *Ibam* space group for pressures up to 7 GPa, where there is a transition to an *I*4/*mcm* tetragonal symmetry. The lattice parameter and electronic structure are investigated as functions of pressure. The results show that the atoms in a crystal become closer together under compression, and the interactions between electrons, especially for the valence electrons, are strengthened. The calculated vibrational frequencies at ambient pressure are in agreement with available experimental data. In addition, the pressure-induced frequency shifts for the internal and lattice modes of AgN_3 crystal upon compression are discussed. We find that the hydrostatic compression produces a more significant influence on the intramolecular interaction than on the intermolecular interaction.

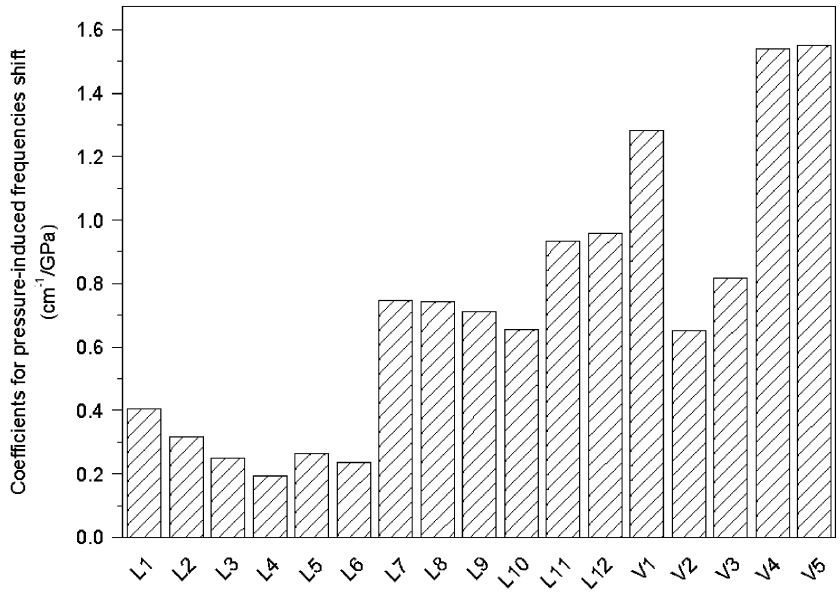

Fig. 7. Coefficients for pressure-induced shifts of vibrational frequencies of the internal modes V1–V5 and lattice modes L1–L12 for AgN_3 from the linear fit of the GGA results in the pressure range of 0–500 GPa.

Acknowledgments

This work was partly supported by National Natural Science Foundation of China (Grant No. 10576016) and "973" Project. W.H. Zhu is grateful for the funding from the School of Chemical Engineering and NJUST.

References

[1] H.D. Fair, R.F. Walker, Physics and Chemistry of the Inorganic Azides, Energetic Materials, vol. 1, Plenum Press, New York, 1977.
[2] W.E. Garner, Chemistry of the Solid State, Butterworths Scientific Publications, London, 1955.
[3] F.P. Bowden, A.D. Yoffe, Fast Reactions in Solids, Butterworths Scientific Publications, London, 1958.
[4] B.L. Evans, A.D. Yoffe, P. Gray, Chem. Rev. 59 (1959) 515.
[5] A.D. Yoffe, in: C.B. Colburn (Ed.), Developments of Inorganic Nitrogen Chemistry, Elsevier, New York, 1996, p. 92.
[6] D.A. Young, Decomposition of Solids, Pergamon Press, Oxford, 1966.
[7] P. Gray, T.C. Waddington, Proc. R. Soc. London A 235 (1956) 106.
[8] P. Gray, T.C. Waddington, Proc. R. Soc. London A 241 (1956) 110.
[9] A.C. Mclaren, G.T. Rogers, Proc. R. Soc. London A 240 (1957) 484.
[10] B.L. Evans, A.D. Young, Proc. R. Soc. London A 250 (1959) 568.
[11] V.R. Pai Verneker, J. Phys. Chem. 72 (1968) 1733.
[12] Yu.A. Zakharov, A.E. Cherkashin, L.V. Kolesnikov, S.V. Koshcheev, Russ. Phys. J. 18 (1975) 786.
[13] T.B. Tang, M.M. Chaudhri, Phys. Rev. B 30 (1984) 6154.
[14] C.S. Rees, M.M. Chaudhri, J. Phys. C: Solid State Phys. 20 (1987) 4097.
[15] Yu.Yu. Sidorin, S.I. Kurakin, V.G. Dodonov, Combust. Explos. Shock Waves 24 (1988) 359.
[16] A.B. Gordienko, Yu.N. Zhuravlev, A.S. Poplavnoi, Russ. Phys. J. 35 (1992) 130.
[17] H.-M. Xiao, Y.-F. Li, J.-J. Qian, Acta Phys. Chim. Sin. 10 (1994) 235.
[18] H.-M. Xiao, Y.-F. Li, Sci. China B 38 (1995) 538.
[19] H.-M. Xiao, Y.-F. Li, Banding and Electronic Structures of Metal Azides, Science Press, Beijing, 1996, p. 88 (in Chinese).
[20] B.P. Aduev, É.D. Aluker, G.M. Belokurov, Yu.A. Zakharov, A.G. Krechetov, J. Exp. Theor. Phys. 89 (1999) 906.
[21] T.M. Klapötke, C.M. Rienäcker, Propell. Explos. Pyrot. 26 (2001) 43.
[22] E.D. Aluker, Yu.N. Zhuravlev, V.Yu. Zakharov, N.G. Kravchenko, V.I. Krasheninin, A.S. Poplavnoi, Russ. Phys. J. 46 (2003) 855.
[23] A.B. Gordienko, A.S. Poplavnoi, Russ. Phys. J. 47 (2004) 1056.
[24] V.I. Oleshko, V.I. Korepanov, V.M. Lisitsyn, V.P. Tsypilev, Tech. Phys. Lett. 30 (2004) 937.
[25] X.H. Ju, G.F. Ji, L. Qiu, H.-M. Xiao, Chem. J. Chin. Univ. 26 (2005) 2125.
[26] D.D. Dlott, M.D. Fayer, J. Chem. Phys. 92 (1990) 3798.
[27] A. Tokmanoff, M.D. Fayer, D.D. Dlott, J. Phys. Chem. 97 (1993) 1901.
[28] C.M. Tarver, J. Phys. Chem. A 101 (1997) 4845.
[29] E.F.C. Byrd, G.E. Scuseria, C.F. Chabalowski, J. Phys. Chem. B 108 (2004) 13100.
[30] B.M. Rice, E.F.C. Byrd, J. Mater. Res. 21 (2006) 2444.
[31] M.D. Segall, P.J.D. Lindan, M.J. Probert, C.J. Pickard, P.J. Hasnip, S.J. Clark, M.C. Payne, J. Phys.: Condens. Matter 14 (2002) 2717.
[32] D. Vanderbilt, Phys. Rev. B 41 (1990) 7892.
[33] G. Kresse, J. Furthmüller, Phys. Rev. B 54 (1996) 11169.
[34] R. Fletcher, Practical Methods of Optimization, vol. 1, Wiley, New York, 1980.
[35] J.P. Perdew, Y. Wang, Phys. Rev. B 45 (1992) 13244.
[36] J.P. Perdew, J.A. Chevary, S.H. Vosko, K.A. ackson, M.R. Pederson, D.J. Singh, C. Fiolhais, Phys. Rev. B 46 (1992) 6671.
[37] H.E. Marr, H. Stanford, Acta Crystallogr. 15 (1962) 1313.
[38] H.G. Pfeiffer, Thesis, California Institute of Technology, 1948.
[39] D. Sanchez-Portal, E. Artacho, J.M. Soler, Solid State Commun. 95 (1995) 685.
[40] M.D. Segall, R. Shah, C.J. Pickard, M.C. Payne, Phys. Rev. B 54 (1996) 16317.
[41] X. Gonze, Phys. Rev. B 55 (1997) 10337.
[42] W. Zhu, J. Xiao, H. Xiao, Chem. Phys. Lett. 422 (2006) 117.
[43] M.I. Eremets, M.Yu. Popov, I.A. Trojan, V.N. Denisov, R. Boehler, R.J. Hemley, J. Chem. Phys. 120 (2004) 10618.
[44] W. Zhu, J. Xiao, H. Xiao, J. Phys. Chem. B 110 (2006) 9856.
[45] W. Zhu, H. Xiao, J. Comput. Chem. (2008), in press.
[46] J.W. Mitchell, Rep. Prog. Phys. 20 (1957) 433.
[47] J.J. Gilman, J. Appl. Phys. 50 (1979) 4059.
[48] J.J. Gilman, Philos. Mag. Lett. 77 (1998) 79.
[49] J.J. Gilman, Philos. Mag. B 67 (1993) 207.
[50] J.J. Gilman, Mech. Mater. 17 (1994) 83.
[51] T. Luty, P. Ordon, C.J. Eckhardt, J. Chem. Phys. 117 (2002) 1775.
[52] M.M. Kuklja, E.V. Stefanovich, A.B. Kunz, J. Chem. Phys. 112 (2000) 3417.
[53] J.I. Bryant, R.L. Brooks, J. Chem. Phys. 54 (1971) 5315.
[54] V.K. Dehnicke, Z. Anorg. Allg. Chem. 409 (1974) 311.